

Reduced Chemical Kinetic Mechanisms: Simulation of Turbulent Non-Premixed CH₄-Air Flame

Guessab Ahmed ^{a*}, Aris Abdelkader ^b, Abdelhamid Bounif ^c, Iskander Gökalp ^d

^a Laboratoire de l'Innovation des Produits et Systèmes Industriels (IPSILab), Département de Génie Mécanique, ENP d'Oran, Oran 31000

^{b,c} Laboratoire des Carburants Gazeux et Environnement, Département de Mécanique, USTOMB d'Oran, Oran 31000.

^d Laboratoire de Combustions et Système Réactifs, CNRS, 45071 Orléans, France.

Abstract

Natural gas is the primary fuel for industrial gas turbines. Although natural gas is mostly Methane, its composition varies. The size of the detailed chemical kinetic model is too large to be used in CFD-Fluent code. The aim of this study is to reduce the number of species and reactions to get a mechanism small enough to use in Fluent. An 8-species reduced mechanism was successfully implanted into the Fluent.

© 2014 Jordan Journal of Mechanical and Industrial Engineering. All rights reserved

Keywords: Natural-Gas, Chemical Reactions, EDC, CFD-Fluent .

1. Introduction

Combustion plays an important role in many industrial applications because it is the main source of producing power and energy. Also, from an environmental point of view, emission of pollutants, due to combustion, causes significant health problems. Therefore, the study of combustion is an important issue for many investigators. Since experimental investigation of combustion is expensive, numerical simulation has been used for decades. Numerical methods have become powerful tools to simulate complex combustion processes and to understand the physics involved. For simulation of combustion, Arrhenius model, the eddy-dissipation concept models are widely used in CFD. One of the most practical models is the eddy-dissipation concept model because it is easy to implement and its results are acceptable for premixed and non-premixed flames. In the eddy-dissipation concept model, every reaction is the same and the model takes into account the turbulent rate only. Therefore, the model should be used only for one-step global reaction and it cannot predict radical species. Multi-step chemical mechanisms are based on Arrhenius rates, and the Arrhenius model computes the rate of reaction using Arrhenius expressions. The Arrhenius model is exact for laminar flames, but is inaccurate for turbulent flames, because this model ignores turbulent fluctuations that are effective on the rate of reaction, temperature, and concentration of pollutants.

Oxidation of methane is perhaps the most important combustion reaction because the main component of natural gas is methane and its combustion is of great

economical importance. Several reaction mechanisms have been developed for the description of methane combustion. The combustion is now one of the major processes to produce energy, whether it is starting from coal, oil or gas. Methane is the simplest hydrocarbon fuel available; several studies have focused on Methane/Air flames. The oxidation of methane is quite well understood and various detailed reaction mechanisms are reported in literature [1;2]. They can be divided into full mechanisms, skeletal mechanisms, and reduced mechanisms. The various mechanisms differ with respect to the considered species and reactions. However, considering the uncertainties and simplifications included in a turbulent flame calculation, the various mechanisms agree reasonably well [3].

In literature, several mechanisms of methane combustion exist. We can cite, for detailed mechanisms: Westbrook [4], Glarborg *et al.* [5], Miller and Bowman [6], and, recently, Konnov v.0.5 [7], Huges *et al.* [8], LCSR [9], Leeds v.1.5 [10], San Diego [11] and the standard GRI-Mech v.3.0 and GRI-Mech v.1.2 [12]; for reduced mechanisms: Westbrook and Dryer [13], and Jones and Lindstedt [14] (more than 2 global reaction); for skeletal mechanisms: Kazakov and Frenklach [15], Yungster and Rabinowitz [16], Petersen and Hanson [17], Hyer *et al.* [18] and Li and Williams [19].

The need to use reduction techniques detailed mechanisms to reduce the computation time and memory allocated by reducing the number of species by reducing the stiffness of the system of differential equations while retaining some predictive qualities of the mechanism. It involves identifying and eliminating non-first important species and then significant reactions. Several studies have focused on the turbulent combustion: M. Cannon *et al.*

[20] numerically studied a diffusion flame of methane with a reaction mechanism reduced from five elementary reactions, deduced from GRI-Mech 2.11 [12]. M. Jazbec *et al.* [21] conducted a numerical study based on a new model developed for the hydrodynamic chemical reaction mechanism with 16 species and 28 reactions. The effectiveness reduced in combustion mechanisms is also emphasized by A. L. Sanchez *et al.* [22].

The present work is focused on the simulation of turbulent confined non-premixed flame of Natural gas. The reduced chemical kinetics scheme of Hyer was used to describe the combustion process in terms of eight chemical reaction equation and 8 species (CH_4 , H_2 , CO , CO_2 , H_2O , O_2 , C_2H_6 and N_2), using the commercial code CFD fluent v6. Some modifications of the usually adopted models for the representation of the turbulence-kinetics interaction are introduced.

2. Problem Description

The numerical model proposed for this study is based on the geometry and dimensions of the experimental jet in co-flow burner used by Lewis and Smoot [23]. The experimental burner geometry for this test is a cylindrical combustor with coaxial injectors, where the primary tube and the air through the secondary annulus inject the natural gas. The total pressure of the combustor is 94 KPa. In the fuel stream, the uniform inlet gas velocity is 21.3 m/s and the mass flow rate is 2.982 g/s, with a temperature of 300 K. Table 1 lists the experimental conditions. The fuel jet consists of 71.8% CH_4 , 11.4% C_2H_6 , 3.6% N_2 , 3 % CO_2 , 0.2% H_2 and 10% Ar. In the air stream, the uniform inlet air velocity is 29.9 m/s and the mass flow rate is 36.3 g/s, with a preheated temperature of 589 K. The average Reynolds number at the chamber inlet results in 17900. Due to the symmetry of the burner, a geometrically simplified axisymmetric computational model was constructed to simulate the burner. The computational domain started at the exit plane of the burner, and extended 1.525m downstream across the axial direction and 10.16cm across the radial direction. The equivalent axisymmetric constructed computational model is shown in Figure 1.

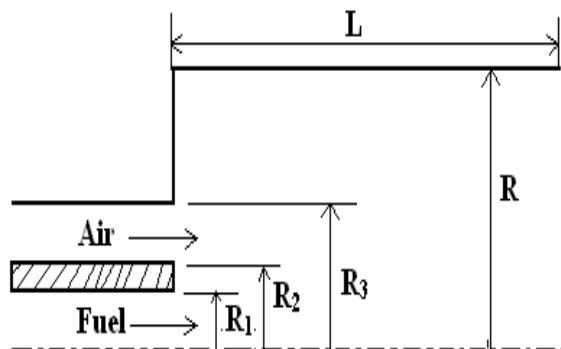


Figure 1. Sketch of the computational domain [23].
($R_1=0.8\text{cm}$, $R_2=1.11\text{cm}$, $R_3=2.86\text{cm}$, $R=10.16\text{cm}$, $L=1.525\text{m}$)

3. Numerical Modeling

3.1. Government Equations

Balance equations for the mean quantities in RANS simulations are obtained by averaging the instantaneous governing equations. This averaging procedure introduces unclosed quantities that have to be modeled by using turbulent combustion models. Using the Favre averages formalism, the averaged balance equations become [24]:

$$\frac{\partial}{\partial x_i} (\bar{\rho} \tilde{u}_i) = 0 \quad (1)$$

$$\frac{\partial}{\partial x_i} (\bar{\rho} \tilde{u}_i \tilde{u}_j) + \frac{\partial \bar{p}}{\partial x_j} = \frac{\partial}{\partial x_i} (\bar{\tau}_{ij} - \bar{\rho} \tilde{u}_i \tilde{u}_j) \quad (2)$$

$$\frac{\partial}{\partial x_i} (\bar{\rho} \tilde{u}_i \tilde{Y}_k) = \frac{\partial}{\partial x_i} \left(\left(\frac{\mu}{Sc_k} + \frac{\mu_t}{Sc_t} \right) \frac{\partial \tilde{Y}_k}{\partial x_j} + \bar{\rho} D_k \frac{\partial \tilde{Y}_k}{\partial x_j} \right) + \bar{R}_i \quad (3)$$

$$\frac{\partial}{\partial x_i} (\bar{\rho} \tilde{u}_i \tilde{h}) = \frac{\overline{DP}}{Dt} + \frac{\partial}{\partial x_i} \left(\frac{\mu}{Pr} \frac{\partial \tilde{h}}{\partial x_i} - \bar{\rho} \tilde{u}_i \tilde{h} \right) \quad (4)$$

In Eq. 3, the thermal diffusion (Soret effect) and the pressure diffusion are neglected. In this work it is assumed that S_{ck} (Schmidt number) is unity which means that the effective specie diffusivity is equal to the viscosity.

3.2. Turbulence Modeling

The standard ($k-\varepsilon$) model (including a correction for round jets performed by using the Pope formulation) turbulence closure model is adopted. In the $k-\varepsilon$ model, the Reynolds stress is closed using mean velocity gradients employing Boussinesq hypothesis. The Reynolds stresses tensor:

$$\overline{\rho u_i'' u_j''} = \frac{2}{3} \bar{\rho} k \delta_{ij} - \mu_t \left(\frac{\partial \tilde{u}_i}{\partial x_j} + \frac{\partial \tilde{u}_j}{\partial x_i} - \frac{2}{3} \delta_{ij} \frac{\partial \tilde{u}_k}{\partial x_k} \right) \quad (5)$$

The turbulent fluxes of species and enthalpy can be closed with a gradient-diffusion hypothesis with the relations:

$$\overline{\rho u_i'' Y_k''} = - \frac{\mu_t}{Sc_{t,k}} \frac{\partial \tilde{Y}_k}{\partial x_i} \quad (6)$$

$$\overline{\rho u_i'' h''} = - \frac{\mu_t}{Pr_t} \frac{\partial \tilde{h}}{\partial x_i} \quad (7)$$

Where, $S_{ct,k}$, and Pr_t are the turbulent Schmidt number and the turbulent Prandtl number, accordingly. Jones and Launder (1972) [25] devised the standard $k-\varepsilon$ model, in which they define the turbulent kinematic viscosity as well as the transport equations for turbulent kinetic energy and turbulent kinetic energy dissipation rate, ε :

$$\mu_t = C_\mu \bar{\rho} \frac{\tilde{k}}{\varepsilon_t} \quad (8)$$

$$\frac{\partial}{\partial x_i} (\bar{\rho} \tilde{u}_i k) = \frac{\partial}{\partial x_i} \left[\left(\mu + \frac{\mu_t}{\sigma_k} \right) \frac{\partial k}{\partial x_i} \right] + P_k + G - \bar{\rho} \varepsilon \quad (9)$$

$$\frac{\partial}{\partial x_i} (\overline{\rho \tilde{u}_i \varepsilon}) = \frac{\partial}{\partial x_i} \left[\left(\mu + \frac{\mu_t}{\sigma_\varepsilon} \right) \frac{\partial \varepsilon}{\partial x_i} \right] + C_{\varepsilon 1} \frac{\varepsilon}{k} (P + C_{\varepsilon 3} G) - C_{\varepsilon 2} \overline{\rho} \frac{\varepsilon^2}{k} + P_{PC} \quad (10)$$

Where G is the turbulent kinetic energy production terms due to buoyancy effect, which are neglected in the present numerical model. The turbulent energy production tensor due to the mean velocity gradients, P_k , is given by

$$P_k = -\overline{u_i'' u_j''} \frac{\partial \tilde{u}_i}{\partial x_j} \quad (11)$$

In the case of a jet flame, a correction is necessary to accurately predict the spreading rate of the jet. This is performed by using the Pope correction, P_{PC} , as an additional term in the equation of turbulence dissipation rate (ε):

$$P_{PC} = \overline{\rho} C_{\varepsilon 3} \frac{\varepsilon^2}{k} S_\varepsilon \quad (12)$$

The term S_ε can be written as (Pope, 1978) [23]:

$$S_\varepsilon = \omega_{ij} \omega_{jk} S_{ij} \quad (13)$$

Where:

$$S_{ij} = \frac{1}{2} \frac{k}{\varepsilon} \left(\frac{\partial u_i}{\partial x_j} + \frac{\partial u_j}{\partial x_i} \right) \quad (14)$$

$$\omega_{ij} = \frac{1}{2} \frac{k}{\varepsilon} \left(\frac{\partial u_i}{\partial x_j} - \frac{\partial u_j}{\partial x_i} \right) \quad (15)$$

Where: $C_{\varepsilon 3} = 0.79$.

The standard values for the model constants (Lauder and Sharma (1974) have been chosen) are:

$$C_\mu = 0.09, C_{\varepsilon 1} = 1.44, C_{\varepsilon 2} = 1.92, \sigma_k = 1.0, \sigma_\varepsilon = 1.3$$

4. Turbulence Combustion Interaction

4.1. Eddy Dissipation Concept (EDC)

The description of the turbulence-chemistry interactions represents one of the most difficult tasks in turbulent combustion; it is necessary to adopt a robust model that accounts for both the chemistry and the turbulence such as the EDC model. Not to be confused with the well known Eddy Dissipation model [26], the eddy-dissipation-concept (EDC) model is an extension of the eddy-dissipation model to include detailed chemical mechanisms in turbulent flows. It assumes that the reaction occurs in small turbulent structures, called the fine scales. The length fraction of the fine scales, γ is modeled as:

$$\gamma = 2.1377 \left(\frac{v \varepsilon}{k^2} \right)^{1/4} \propto \text{Re}_t^{-1/4} \quad (16)$$

Where, the volume fraction constant = 2.1377, and v is the kinematic viscosity. Species are assumed to react in the fine structures over a time scale τ , which is proportional to the kolmogorov time scale:

$$\tau = 0.4082 \sqrt{\frac{v}{\varepsilon}} \propto t_{Kolmogorov} \quad (17)$$

The time scale constant is equal to 0.4082. This constant can be adjusted in FLUENT either to accelerate or slow down the reaction. Decreasing the time scale constant will result in an acceleration of the reaction while increasing it slows down the reaction process. FLUENT assumes that the combustion at the fine scales proceeds as a constant pressure reactor, where * denotes fine-scale quantities:

$$\frac{dY_k^\bullet}{dt} = \frac{\overline{\omega}_k}{\rho^\bullet} \quad (18)$$

With the initial conditions taken as the current species and temperatures in the cell. Initial condition:

$Y_k^* = Y_k$. Y_k^* is the fine scale species mass fraction after reacting over time τ . The source term S_k in the general conservation equation for the mean species i is modeled as:

$$S_K = \frac{\gamma^2}{\tau} (Y_k^\bullet - Y_k) \quad (19)$$

4.2. Chemical Reaction Mechanism for Natural Gas

In this study, the Hyer mechanism often used in combustion modeling of natural gas (Table 1), is an eight-step reaction for reversible.

Table 1. Hyer chemical kinetics mechanism and Arrhenius rate coefficients [18].

| Reaction | A_k | E_k [J/Kmol] | β_k |
|---|----------|----------------|-----------|
| $\text{CH}_4 + 0.5\text{O}_2 \rightarrow \text{CO} + 2\text{H}_2$ | 4.40e+09 | 1.26e+08 | 0 |
| $\text{CH}_4 + \text{H}_2\text{O} \rightarrow \text{CO} + 3\text{H}_2$ | 3.00e+08 | 1.26e+08 | 0 |
| $\text{CO} + \text{H}_2\text{O} \rightarrow \text{CO}_2 + \text{H}_2$ | 2.75e+10 | 8.37e+07 | 0 |
| $\text{CO}_2 + \text{H}_2 \rightarrow \text{CO} + \text{H}_2\text{O}$ | 9.62e+10 | 1.26e+08 | -0.85 |
| $\text{H}_2 + 0.5\text{O}_2 \rightarrow \text{H}_2\text{O}$ | 7.45e+13 | 1.67e+08 | -0.91 |
| $\text{H}_2\text{O} \rightarrow \text{H}_2 + 0.5\text{O}_2$ | 3.83e+14 | 4.12e+08 | -1.05 |
| $\text{C}_2\text{H}_6 + \text{O}_2 \rightarrow 2\text{CO} + 3\text{H}_2$ | 4.20e+11 | 1.25e+08 | 0 |
| $\text{C}_2\text{H}_6 + 2\text{H}_2\text{O} \rightarrow 2\text{CO} + 5\text{H}_2$ | 3.00e+08 | 1.25e+08 | 0 |

In general, a chemical reaction can be written in the form as follows:

$$\sum_{i=1}^N v'_{i,k} A_i \Leftrightarrow \sum_{i'=1}^N v''_{i',k} A_{i'} \quad (20)$$

Where:

N = number of chemical species in the system

$v'_{i',k}$ = Stoichiometric coefficient for reactant i in reaction k

$v''_{i',k}$ = Stoichiometric coefficient for product i in reaction k

A_i = chemical symbol denoting species i

$k_{f,k}$ = forward rate constant for reaction k

$k_{b,k}$ = backward rate constant for reaction k

Equation 3 is valid for both reversible and non-reversible reactions. For non-reversible reactions, the backward rate constant $k_{b,k}$ is simply omitted. The summations in Eq. 17 are for all chemical species in the system, but only species involved as reactants or products will have non-zero stoichiometric coefficients, species that are not involved will drop of the equation except for third-body reaction species. The mole reaction rate, $\hat{R}_{i',k}$ [$\text{Kmol.m}^{-3}.\text{s}^{-1}$] is determined from Eq. 18.

$$\hat{R}_{i',k} = \frac{d[C_j]}{dt} \Gamma (v''_{i,k} - v'_{i,k}) \left(k_{f,k} \prod_{j=1}^N [C_j]^{\eta'_{j,k}} - k_{b,k} \prod_{j=1}^N [C_j]^{\eta''_{j,k}} \right) \quad (21)$$

Where $[C_j] \left[\frac{\text{Kmol}}{\text{m}^3} \right]$ is the mole concentration of

species j in reaction k , $v'_{i,k}$ and $v''_{i,k}$ are the reactant and

product stoichiometric coefficients of species i in reaction k , respectively,

$\eta'_{j,k}$ and $\eta''_{j,k}$ are the rate exponents of the reactant and product j' in reaction k , respectively, Γ is the net effect of third bodies on the reaction rate. This term is given by:

$$\Gamma = \sum_{j'}^N \gamma_{j',k} C_{j'} \quad (22)$$

Where $\gamma_{j',k}$ is the third-body efficiency of the j' th species in the k th reaction. The forward and backward reaction rate constants $k_{f,k}$ and $k_{b,k}$ are usually evaluated with the Arrhenius equation given in Eq. 20.

$$k_{f,k} = A_k T^{\beta_k} \exp(-E_k/RT) \quad (23)$$

Where A_k is the pre-exponential constant of reaction k , T [K] is the temperature, β_k is the temperature exponent of reaction k , E_k [J.Kmol^{-1}] is the activation energy of reaction k and R [$\text{J.Kmol}^{-1}.\text{K}^{-1}$] is the gas constant. The values of $v'_{i,k}$, $v''_{i,k}$, $\eta'_{j,k}$, $\eta''_{j,k}$, β_k , A_k , E_k and $\gamma_{j',k}$ can be provided the problem definition. The mass reaction rate of species j in reaction k , $R_{j,k}$ [$\text{Kg.m}^{-3}.\text{s}^{-1}$] is determined with Eq. 21:

$$R_{j,k} = \bar{R}_{j,k} M_j \quad (24)$$

If the reaction is reversible, the backward rate constant for reaction k using Eq. 22. Unless a distinct reverse reaction is specified. Determination of K_k is discussed by:

$$k_{b,k} = \frac{k_{f,k}}{K_k} \quad (25)$$

Where k_k is the equilibrium constant for the k -th reaction. Computed from:

$$K_k = \exp\left(\frac{\Delta S_k^0}{R} - \frac{\Delta H_k^0}{RT}\right) \left(\frac{P_{atm}}{RT}\right)^{\sum_{k=1}^{NR} (v''_{i,k} - v'_{i,k})} \quad (26)$$

Where P_{atm} denotes atmospheric pressure (101325Pa). The term within the exponential represents the change in Gibbs free energy, and its components are computed as follows:

$$\frac{\Delta S_k^0}{R} = \sum_{i=1}^N (v''_{i,k} - v'_{i,k}) \frac{S_i^0}{R} \quad (27)$$

$$\frac{\Delta H_k^0}{RT} = \sum_{i=1}^N (v''_{i,k} - v'_{i,k}) \frac{h_i^0}{R} \quad (28)$$

Where S_i^0 and h_i^0 are, respectively, the standard-state entropy and standard-state enthalpy including heat of formation. FLUENT employs the SI unit system. The values given in Table 5 and 6 are given in the units [cm], [s], [cal] and [mol] must therefore be converted.

5. Simulation Details

The numerical simulation of the flow field includes the solution of the governing equations which consists of Favre-averaged form of continuity, momentum, energy, species conservation, and modified standard k-ε equations. It consists of 8 species and 8 reversible reactions. The standard k-ε turbulence closure model is adopted. The governing equations are solved using the Fluent CFD package modified with User Defined Functions (UDF) in order to integrate the reaction rate formula proposed by Hyer [18]. In Fluent, the differential equations governing the problem are discretized into finite volume and then solved using algebraic approximations of differential equations. SIPMLE algorithm was chosen for the coupling between the velocity and the pressure. For all simulations presented in this paper, a First Order Upwind Scheme was used for the conservation equation of momentum, turbulent kinetic energy, turbulent dissipation rate, mean mixture fraction. The Standard scheme was used for interpolation methods of pressure. This means that the solution approximation in each finite volume was assumed to be linear. This saved computational expenses. In order to properly justify using a first order scheme, it was necessary to show that the grid used in this work had adequate resolution to accurately capture the physics occurring within the domain. In other words, the results needed to be independent of the grid resolution. This was verified by running simulations with higher resolution grids. In a reacting flow, such as that studied in this work, there are significant time scale differences between the general flow characteristics and the chemical reactions. The criterion of convergence is the summation of residual mass sources less than 10^{-3} for the other terms of the transport equations and is 10^{-6} for energy equation. The computational space seen in Figure 1 given a finite volume mesh is divided by a staggered non-uniform quadrilateral cell (Figure 2). A total number of 5600 quadrilateral cells were generated using non-uniform grid spacing to provide an adequate resolution near the jet axis and close to the burner where gradients were large. The grid spacing increased in radial and axial directions since gradients were small in the far-field. The combustion will be modeled using a reduced 8-step reaction mechanism scheme, and the radiative heat transfer of the diffusion flame is calculated with the *P1* model [24]. The density is obtained from the ideal gas law. The interaction between turbulence and chemistry is often handled through the

Eddy-Dissipation Concept (EDC). The controlling rate is assumed to be the slower between the kinetic values and turbulent mixing rate. The specific heat values for the species are defined as piecewise-polynomial function of temperature. The options used in this work are presented in Tables 2 and 3:

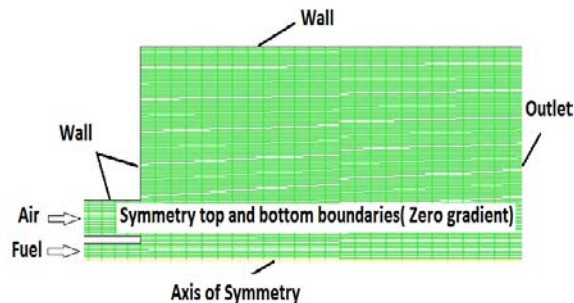


Figure 2. 2D view of the computational domain (Mesh) and boundary conditions.

Table 2. Under-Relaxation factors

| | |
|---|-----|
| Pressure | 0.3 |
| Density | 0.5 |
| Body Forces | 1 |
| Momentum | 0.7 |
| Turbulent Viscosity | 0.9 |
| Species Concentration Y_i | 0.9 |
| Energy E | 0.4 |
| Turbulent kinetic energy 'k' | 0.8 |
| Turbulent dissipation rate ' ϵ ' | 0.8 |

Table 3. Discretization and computational model step.

| | |
|----------------------------|----------------------------|
| Solver Type | Pressure Based |
| Viscous Model | Turbulent (k- ϵ) |
| 2D-Space | Axisymmetric |
| Pressure-Velocity Coupling | SIMPLE |
| Pressure | Standard |
| Momentum Equations | First Order Upwind |
| Species Equations | First Order Upwind |
| Energy Equation | First Order Upwind |
| Turbulent kinetic Energy | First Order Upwind |
| Turbulent Dissipation Rate | First Order Upwind |

6. Results and Discussions

In this section, we present simulation results and we compare them with the experimental data. In this study, we discuss predictions of the mass fraction of all species. Finally, we analyze the predictions of mean temperature. The sensitivity of the predictions to the choice of k- ϵ model ($C_{\epsilon 3} = 0.79$), chemical kinetic mechanism and the EDC model for turbulence-chemistry interaction is studied. The reduced mechanism of Hyer was previously validated on the basis of non-premixed flames. Then, the mechanism implemented into the CFD code Fluent, using the method of directed relation graph and Quasi Steady State Assumption. The mechanism was incorporated into the Fluent by the means of a user-defined function that

uses the subroutine (Define-Net-Reaction-Rates) to compute the species reaction rates, which are fed into the turbulence-combustion model. The FORTRAN subroutine is linked to Fluent through the (DNRR) argument macro. This macro is called the EDC model and used to compute the closed turbulent species reaction rates. The EDC uses the FORTRAN reactions rates as an input to the turbulent reaction rates. In this manner, the UDF is a complement to the EDC model and does not by-pass the EDC model. Once the reduced mechanism is constructed and executed, the subroutine that computes the chemical source terms is automatically generated. A coupled set of nonlinear Quasi Steady State species equations are numerically solved within the subroutine to provide the necessary elementary reaction rates for the reduced mechanism. This subroutine, which is compatible with FLUENT, is specified in the user-defined function and returns the molar production rates of the species given the pressure, temperature, and mass fractions. The Under-relaxation factors are different for different variables, varying from 0.3 to 0.9. The energy equation is very difficult to converge, so the factor is taken as 0.4. The inlet turbulent specification method is 'intensity and length scale'. Turbulence intensity is 10% and turbulence length scales are 0.008 m for fuel and 0.0175 m for air. We begin by comparing the computational cost of Hyer mechanism and the global mechanism model [13], in terms of the average CPU (execution) time per time step. The relative elapsed CPU times are compared in Table 4.

Table 4. Average execution time per time step.

| Kinetic model | Species | Reaction | CPU [s] | Iter. |
|---------------|---------|----------|---------|-------|
| 1-step | 04 | 01 | 0.00596 | 1635 |
| 8-step | 08 | 08 | 0.0854 | 15356 |

In the 8-step mechanism, more reaction equations are computed, then more CPU time is spent and it becomes more difficult to converge. In general, the computational cost increases with the number of reaction-step and species and it becomes more difficult for convergence. Figures 4 and 5 show the contour plot of the temperature fields from the simulation using the Global and Hyer mechanisms.

It is noticed that the smallest flame is predicted by the 1-step scheme, whereas the largest flame is predicted by the 8-step model. It is observed that the predicted maximum temperature calculated for the turbulent diffusion flame, using different chemical kinetic schemes for 1-step model, is 2960 K, but in the 8-step scheme, it is 2680 K. The 1-step mechanism assumes that the reaction products are CO_2 and H_2O , the total heat of reaction is over predicted.

In the actual situation, some CO , C_2H_6 and H_2 exist in the combustion products with CO_2 and H_2O . This lowers the total heat of reaction and decreases the flame temperature. The 8-step mechanism includes CO , C_2H_6 and H_2 , so we can get more detailed chemical species distribution.

Radial composition profiles for CH_4 , CO_2 , O_2 , H_2O , CO , H_2 , C_2H_6 and Temperature (K) at several axial locations ($x = 10, 25$ and 50 cm) are shown in Figures 5 to 11, and the test results of Lewis and Smoot are also shown. Those figures show that the calculated results are in good agreement with experimental data.

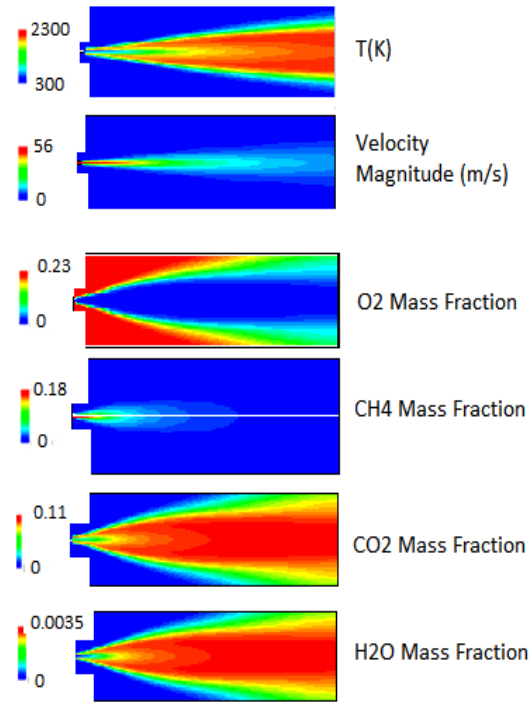


Figure 3. Results of fluent simulation of Non-Premixed CH₄-air flame using a One-step scheme

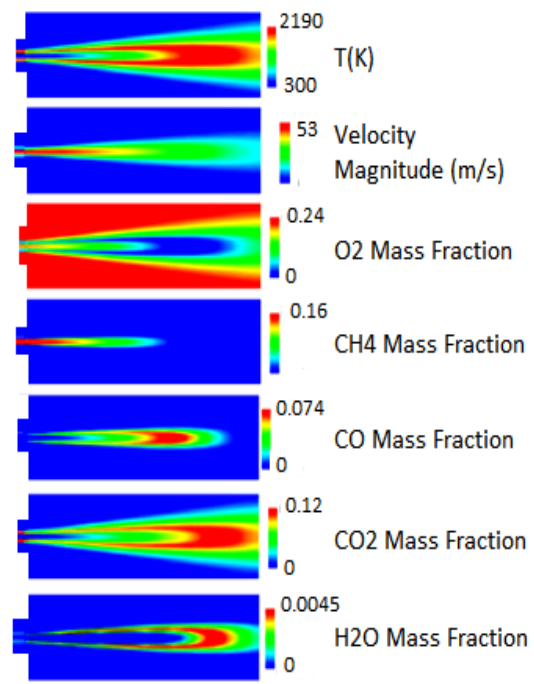


Figure 4. Results of fluent simulation of Non-Premixed CH₄-air flame using an 8-step scheme

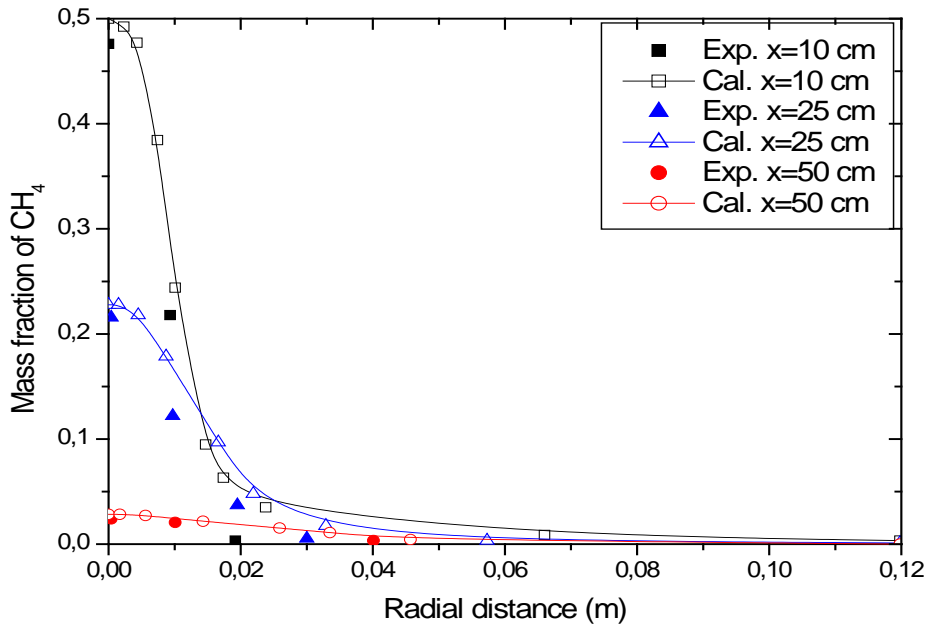


Figure 5. Radial CH₄ mole fraction profiles at several axial locations.

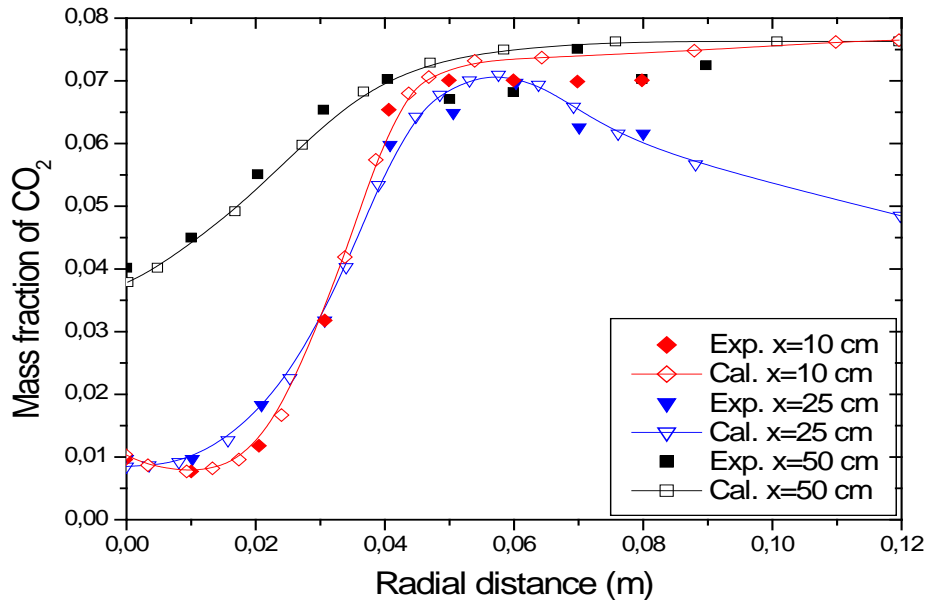


Figure 6. Radial CO₂ mole fraction profiles at several axial locations.

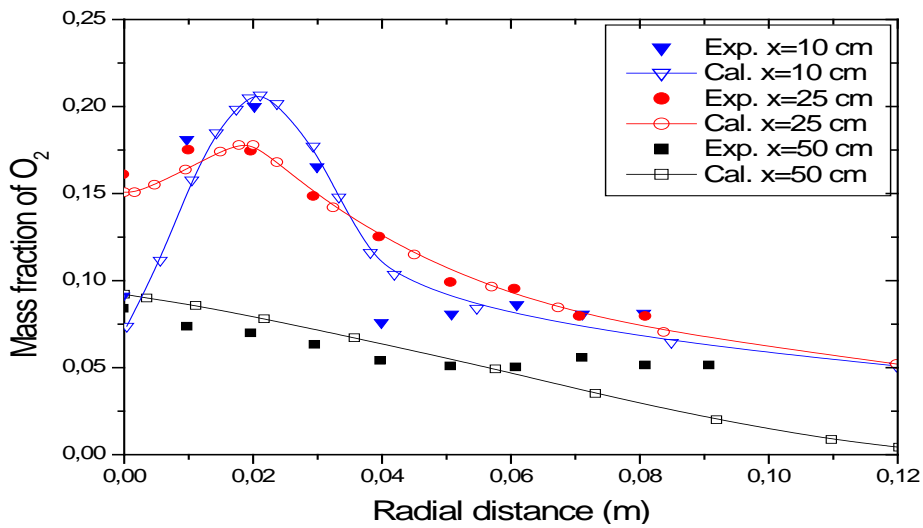


Figure 7. Radial O₂ mole fraction profiles at several axial locations.

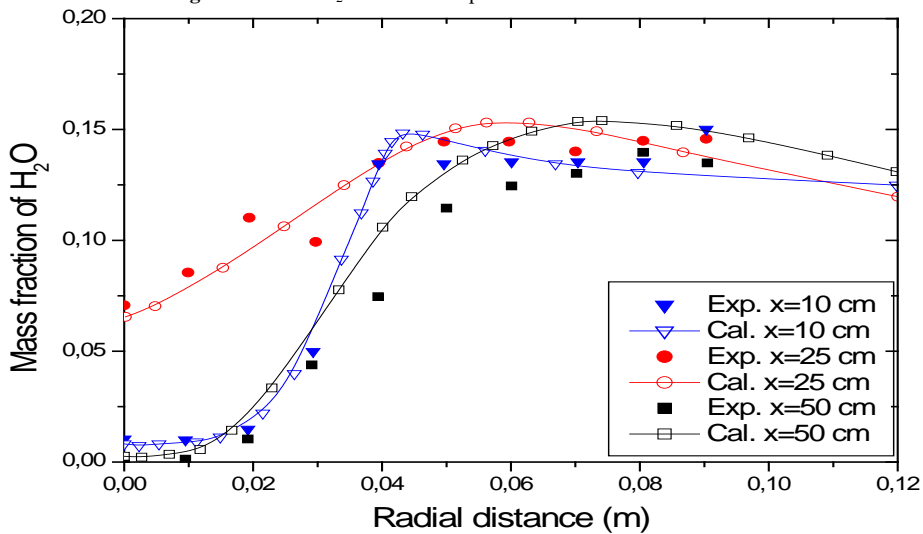


Figure 8: Radial H₂O mole fraction profiles at several axial locations.

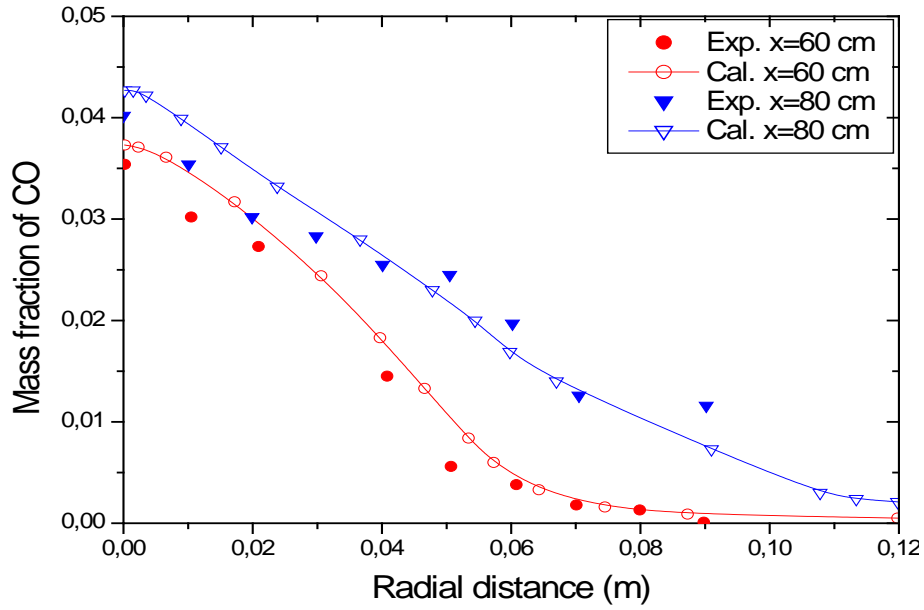


Figure 9. Radial CO mole fraction profiles at several axial locations.

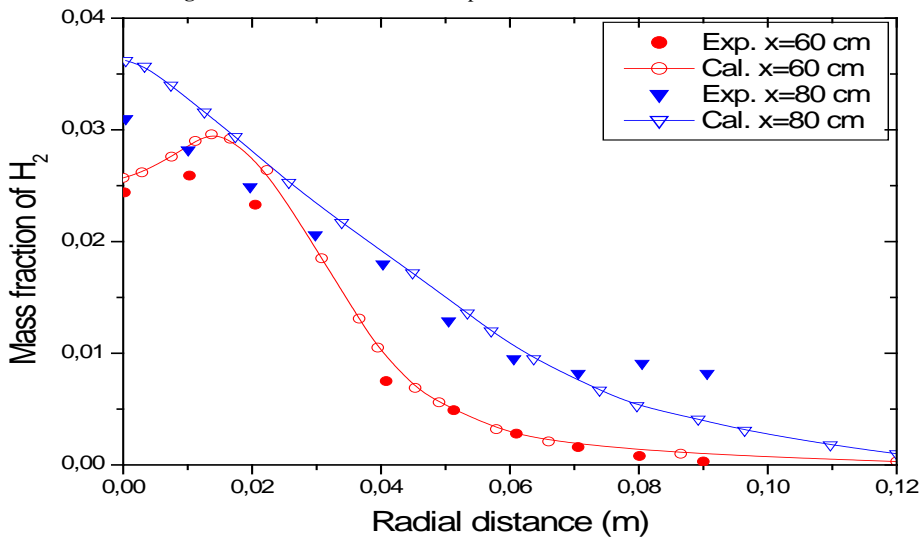


Figure 10. Radial H₂ mole fraction profiles at several axial locations.

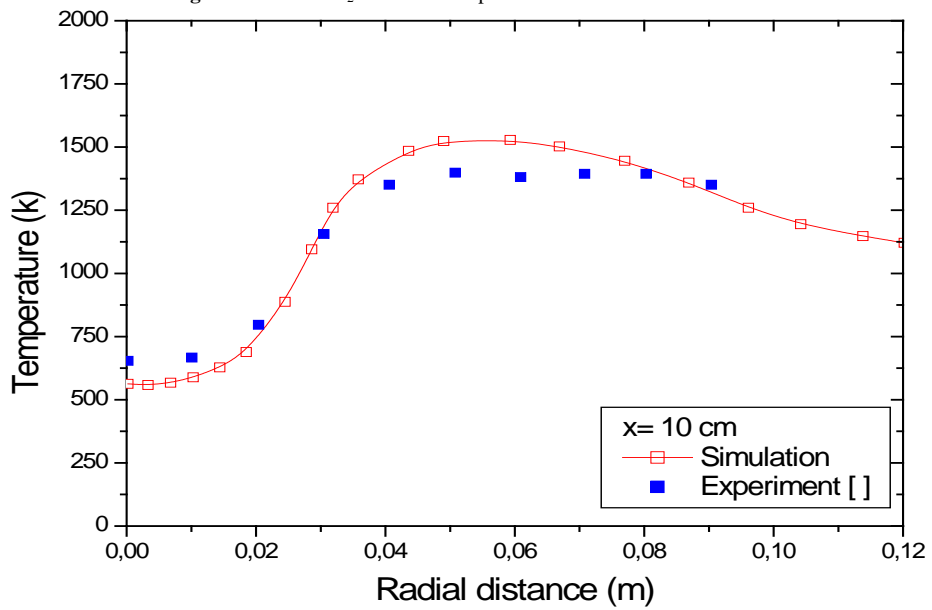


Figure 11. Temperature profile at x=10 cm.

7. Conclusion

The main results are:

- The 8-step reaction mechanism was successfully implanted into the Fluent.
- The Eddy-Dissipation Concept (EDC), which has been successfully used in RANS calculations of turbulent diffusion flames, has been formulated as a combustion model for RANS simulations of turbulent jet diffusion flames. The model has been applied in a simulation natural gas/air flame.
- The results are compared with experimental data for the temperature and various chemical species. The agreement is very reasonable for all quantities.

Future research work is needed to be done on:

- Using a reduced chemical kinetics mechanism for NO_x emission prediction in natural gas combustion.
- Adoption of more reasonable turbulence-chemistry model interaction for multi-step chemical reaction equations.

References

- [1] Simmie J. M. (2003), detailed chemical kinetic models for the combustion of hydrocarbon fuels, *Progress in Energy and Combustion Science*, Vol. 29, p. 599-634.
- [2] Guessab A., Aris A.E.K, Bounif A. and Gokalp I., Numerical Analysis of Confined Laminar Diffusion Flame: Effects of Chemical Kinetic Mechanisms, *Int. J. of Advanced Research in Engineering and Technology*, Vol. 4, January, pp. 59-78, (2013).
- [3] Davidenko D. M., Gökalp I., Dufour E., Magre P. (2005), Numerical simulation of supersonic combustion with CH₄-H₂ fuel, *European Conference for Aerospace Sciences (EUCASS)*, Moscow, Russia, 4-7 July.
- [4] Westbrook, C. K., Applying Chemical Kinetics to Natural Gas Combustion Problems, Report No. PB-86-168770/XAB, Lawrence Livermore National Laboratory, Livermore, Cal., USA, (1985).
- [5] Glarborg, P., Miller, J. A., Kee, R. J., Kinetic Modeling and Sensitivity Analysis of Nitrogen Oxide formation in Well Stirred Reactors, *Combustion and Flame*, 65 (1986), 2, pp. 177-202
- [6] Miller, J. A., Bowman, C. T., Mechanism and Modeling of Nitrogen Chemistry in Combustion, *Progress in Energy and Combustion Sciences*, 15 (1989), 4, pp. 287-338.
- [7] Konnov, A. A., Detailed Reaction Mechanism for Small Hydrocarbons Combustion, (2000) Release 0.5, <http://homepages.vub.ac.be/~akonnov/>
- [8] Huges, K. J., et. al., Development and Testing of a Comprehensive Chemical Mechanism for the Oxidation of Methane, *International Journal of Chemical Kinetics*, 33 (2001), 9, pp. 515-538.
- [9] Dagaut P. (2002), on the kinetics of hydrocarbon oxidation from natural gas to kerosene and diesel fuel, *Phys. Chem. Chem. Phys.*, Vol. 4, p. 2079-2094.
- [10] The Leeds methane oxidation mechanism, <http://www.chem.leeds.ac.uk/Combustion/methane.htm>.
- [11] San Diego Mechanism 2003/08/30, <http://maemail.ucsd.edu/~combustion/cermech/oldversions/sandiego20030830/>
- [12] GRI-Mech v.3.0, http://www.me.berkeley.edu/gri_mech.
- [13] Westbrook, C. K., Dryer, F. L., Simplified Reaction Mechanisms for the Oxidation of Hydrocarbon Fuels in *Flames, Combustion Sciences and Technologies*, 27(1981), 1-2, pp. 31-43.
- [14] Jones, W. P., Lindstedt, R. P., Global Reaction Schemes for Hydrocarbon Combustion, *Combustion and Flame*, 73 (1988), 3, pp. 233-249.
- [15] Kazakov A., Frenklach M., Reduced Reaction Sets based on GRI-Mech 1.2, <http://www.me.berkeley.edu/drm/>
- [16] Yungster S., Rabinowitz M. J. (1994), Computation of shock-induced combustion using a detailed methane-air mechanism, *Journal of Propulsion and Power*, Vol. 10, No. 5, p. 609-617.
- [17] Petersen E. L., Hanson R. K. (1999), Reduced kinetics mechanisms for ram accelerator combustion, *Journal of Propulsion and Power*, Vol. 15, No. 4, p. 591-600.
- [18] Hyer P., Stocker D. and Clar I.O., Gravitational Effects on Laminar Diffusion Flames, *Creare. X Users' Group Meeting Proceedings*, pp. 345-372, 1991.
- [19] Li S. C., Williams F. A. (2002), Reaction mechanisms for methane ignition, *Journal of Engineering for Gas Turbines and Power*, Vol. 124, p. 471-480.
- [20] S.M. CANNON *et al*, PDF Modeling of lean premixed combustion using in situ tabulated chemistry, *Comb. & Flame* 119:223-252(1999)
- [21] M.Jazbec *et al*, Simulation of the ignition of lean methane mixtures using CFD modeling and a reduced chemistry mechanism, *Elsevier App. Math. Modeling* 24 (2000) 689-696.
- [22] A.L. Sanchez *et al*, The reduced kinetic description of lean premixed combustion, *Comb. & Flame* 123:436-464 (2000).
- [23] Lewis M.H. and Smoot L.D., Turbulent Gaseous Part I: Theory and Local Species Concentration Measurements, *J. of Propulsion and Power*, Vol. 42, pp. 183-196, 2001.
- [24] FLUENT. 2009. "Theory Guide: Release 12.0." Last modified January 23, 2009.
- [25] Jones, W. P., and Launder, B. E. (1972), "The Prediction of Laminarization with a Two-Equation Model of Turbulence", *International Journal of Heat and Mass Transfer*, vol. 15, 1972, pp. 301-314.
- [26] Pope S.B. (1978). An explanation of the turbulent round-jet/plane-jet anomaly, *AIAA Journal*, Vol. 16, No. 3, p. 279-281.
- [27] Magnussen B, Hjertager BH (1976) 16th symposium (int.) on combustion, 719-729, The Combustion Institute, Pittsburgh.